Terahertz Gunn-like oscillations in InGaAs/InAlAs planar diodes

S. Pérez, T. González, D. Pardo and J. Mateos

Departamento de Física Aplicada, Facultad de Ciencias,
Universidad de Salamanca, Plaza de la Merced s/n, 37008 Salamanca, Spain

ABSTRACT:

A microscopic analysis of self-generated Terahertz (THz) current oscillations taking place in planar InAlAs/InGaAs slot-diodes operating under dc bias is presented. An ensemble Monte Carlo (MC) simulation is used for the calculations. The onset of the oscillations is threshold-like, for drain-source voltages surpassing 0.6 V. Gunn-like mechanisms and the modulation of the injection of electrons into the recess-to-drain region, which takes place in the Γ or L valleys alternatively, are found at the origin of the phenomenon. THz frequencies are reached because of the presence of ultra-fast Γ electrons in the region of interest. Extremely high velocities are achieved by (i) the effect of the recess, which focuses the electric field and launches very fast electrons into the drain region, and (ii) the influence of degeneracy, which significantly reduces the rate of scattering mechanisms and enhances the electron mobility in the channel.

PACS numbers: 85.30.Tv, 85.30.Fg

I. INTRODUCTION

THz radiation (100 GHz to 10 THz), also known as T-rays, provides a huge potential in the fields of imaging, ranging, spectroscopy and guidance, that could be of strong interest for a big number of medical, robotics, security and military applications[1]. The THz frequency range lies between microwaves and infrared light in the electromagnetic spectrum and thus, the technology for producing T-ray sources is at the limits of electronics from one side and optical systems from the other. Indeed, no powerful radiation sources have been available until last years[2,3] and, even with the strong advances obtained with quantum cascade lasers (at cryogenic temperatures), nowadays it does not yet exist a compact, room-temperature, high-power source that is well controlled, tunable and suitable for the THz frequency range. From the practical point of view, the most interesting solution seems to be THz sources based on solid state devices, which offer the best possibilities of integration with other electronic or optoelectronic devices within a single chip.[1]

Recent measurements in nanometer gate length InAlAs/InGaAs High Electron Mobility Transistors (HEMTs) have shown the emission of radiation at THz frequencies.[4,5] Initially, the mechanism for THz emission in HEMTs was identified as the result of plasma wave generation due to the Diakonov-Shur instability.[6] However the threshold-like behaviour of THz emission (when increasing the drain bias) and the associated kinks appearing in the I-V curves indicate that, instead of plasma instabilities, a hot carrier mechanism such as Gunn effect could be responsible for those high frequency oscillations.[7,8]

In this work we present a detailed Monte Carlo study of current oscillations in the ungated heterostructures on which these HEMTs are based. For this sake we perform calculations of the current noise spectra, which can give precise indications on the onset of collective phenomena such as plasma or Gunn oscillations. Though this oscillatory behaviour has also been found in nanometer gate length InAlAs/InGaAs HEMTs, ungated HEMT-like heterostructures (also called slot diodes) are chosen for simplicity, because the gate terminal is not essential to originate the oscillations. The fundamental point is the localization of a strong potential drop across a narrow region, effect obtained by means of a recess. We will show that ultra-fast Gunn-like phenomena take place in these planar diodes, leading to current oscillations in the THz range. Gunn oscillations due to the transfer of electrons to the upper valleys in the gate-drain region of HEMTs or in planar AlGaAs/GaAs heterostructures have already been experimentally observed and found in Monte Carlo simulations;[9,10] however, they usually exhibit much lower frequencies. In order to reach oscillation frequencies in the THz range, the high field domain must travel much faster than the saturation velocity of electrons in the channel. This paper proposes the geometry and explains the physics of a novel form of planar ultra-fast Gunn-like diode capable to produce these extremely high frequency oscillations. Remarkably, the topology of this planar two terminal device makes it ideally suited for integration into Monolithic Microwave Integrated Circuits (MMICs) in contrast to conventional Gunn diodes. This fact facilitates the developing of the THz technology towards portable and much less costly systems.

The paper is organized as follows. In Sec. II the physical system under analysis together with the details of the MC simulation are described. In Sec. III the results obtained for the static characteristics and the oscillatory behavior of the diodes are reported. Sec. IV summarizes the main conclusions and future lines of our work.

II. PHYSICAL MODEL AND MONTE CARLO SIMULATION

The layer structure of the simulated slot diodes is shown in Fig. 1. It consists a 200 nm $In_{0.52}Al_{0.48}As$ buffer followed by a 15 nm thick $In_{0.70}Ga_{0.30}As$ channel, three layers of $In_{0.52}Al_{0.48}As$ (a 3 nm spacer, a 6x10^{12} cm^{-2} δ-doping modelled as a 4 nm layer doped at N_D= 1.5x10^{19} cm^{-3} and a 10 nm Schottky layer) and finally a 10 nm thick $In_{0.53}Ga_{0.47}As$ cap (N_D=6x10^{18} cm^{-3}). Note that this layer structure is the base for the realization of real InP based HEMTs.[7,8,10] A key parameter in the geometry of the diode is the recess-to-drain distance, which in the simulated diode is 550 nm.

Calculations are performed by using an ensemble MC simulator at room temperature self-consistently coupled with a 2D Poisson solver. The material parameters and microscopic models are reported in Ref. 11. The devices are divided into 5 nm long and 1 to 10 nm wide meshes depending on the doping and the required resolution of the potential along the structure. Ohmic boundary conditions are considered in the source and drain contacts, which are placed vertically adjacent to different materials.[11] Accordingly, nonuniform potential and concentration profiles are considered along these contacts, those that would be obtained if real top electrodes were simulated.[11]

The effect of degeneracy is accounted for by using locally the classical rejection technique, where the electron heating and nonequilibrium screening effects are introduced by means of the local electron temperature. No other quantum effects are considered in the simulation in order to have reasonable CPU times. The validity of this approximation (especially under high field conditions) and that of the whole Monte Carlo model has been confirmed in previous works.[11,12]

In order to detect and emphasize the presence of plasma or Gunn oscillations, special attention is devoted to the calculation of noise spectra due to their extreme sensitivity to microscopic features of carrier dynamics and the possibility to easily perform a frequency analysis of the electrical fluctuations.

III. RESULTS

The static current-voltage characteristic of the slot diode is shown in Fig. 2. It can be observed that a kink appears just when Γ-L intervalley transfer starts to be important in the InGaAs channel, for V_{DS} about V_{th} = 0.6 V (Γ-L energy separation is 0.61 eV). For voltages above V_{th}, current oscillations (originated, as we will see, by an ultra-fast Gunn-like effect) clearly appear (right inset). These are coherent oscillations that gives birth to a pronounced peak in the current spectrum [as shown in Fig. 2(b)] and also to a decrease the mean value of the current [producing the kink observed in the *I-V* curves, Fig. 1(a)]. Plasma oscillations, appearing for low applied voltages, are non-coherent, but also provide a peak in the current noise spectrum as shown in Fig. 2(c). However this peak is easily distinguished from that provided by Gunn-like oscillations, first because it lies at much higher frequencies, and second, because its amplitude is much lower. These differences are observed in Fig. 3, where the frequency and amplitude of the main peak found in the current noise spectrum are plotted as a function of the applied bias. High amplitude Gunn-like oscillations, with a frequency around 1 THz, appear for $V_{DS} > V_{th}$, while for lower voltages there are only low-amplitude higher-frequency plasma oscillations (around 4.5 THz). The amplitude of these ultra-fast Gunn oscillations increases, saturates and even decreases for the highest voltages (grey circles, left axis) while the frequency (entering the THz range) decreases with increasing bias (grey triangles, right axis). A frequency shift of 0.78 THz is obtained by increasing the bias from 0.6 to 1.3 V. This wide frequency tunability can be very important for practical applications.

Figure 4 shows the profiles of electric field in the channel of the heterostructure at different time moments within one period of the oscillation, for V_{DS} =1.0 V. The presence of a peak in the electric field distribution that displaces along the recess-drain region at extremely high velocity is observed ($v_E \sim 10\text{x}10^7$ cm/s). This increase of the electric field is spatially linked to a low carrier concentration in the channel, as can be observed in Fig. 5(a). Moreover, as observed in Fig. 5(b), which shows the total carrier density (and the Γ and L contributions) at t=0, the region with low concentration is originated by the reduced presence of Γ electrons, with most of the carriers populating the L valley (in a concentration similar to that of the rest of the recess-drain region).

Therefore, the oscillatory behavior of the current must be somehow related to intervalley mechanisms that push carriers into the upper satellite valleys. This fact is analogous to what happens in the typical Gunn diode oscillations. However the creation and annihilation of space-charge domains in the heterostructure slot diodes exhibit important differences with respect to the behavior of classical Gunn devices. The active region for the formation and displacement of the field inhomogeneity is not the total cathode-to-anode distance but only the recess-to-drain region. Indeed, the peak in the electric field at the drain edge of the recess is responsible for the maintenance of oscillations due to the modulation of its height along a period and also for the high speed of the Γ valley electrons injected into the drain region. However, if this peak is sufficiently high (what happens at some moments during one period), it makes electrons gain enough energy to reach the L valley, and almost no fast electron subsists at that point.

To understand the origin of the oscillation it is interesting to observe the profile of the electric potential in the channel at different times within one period as shown in Fig. 6 for an applied voltage of 1.0 V. The point at which a value of 0.6 V (energy distance between Γ and L valleys) is reached is marked by a circle in each curve. Depending of the position at which such a value is reached, electrons are injected into the recess-drain region just in the Γ valley (V_{th} reached after the recess) or in both Γ and L valleys (V_{th} reached at the edge of the recess). Note that due to the low effective mass of electrons in InGaAs and the high carrier concentration in the channel, Γ electrons move quasiballistically along the high-field region under the recess, without dissipating the energy gained from the electric field (very few scattering mechanisms are observed in the simulations).

In the range 0.7-1.0 ps, the carrier concentration is essentially uniform in the recess-drain region (no depleted zone, carriers nearly equally distributed in Γ and L valleys). The most resistive part of the device is the (low-concentration) region under the recess, where a drop of voltage higher than V_{th} takes place. As a consequence, an increasing amount of electrons jump to the L valley near the drain edge of the recess. These electrons are very slow (compared to those in the Γ valley) and need a long time to reach the drain terminal. In contrast, Γ-carriers injected into the drain region prior to the L electrons move very fast towards the contact, leading to a decrease of concentration near the recess, not compensated by new fast electrons injected in the Γ valley (since only L valley electrons are being injected). This produces a partially depleted region where practically only carriers in the L valley are present [see Fig.

5(b)]. This region of low concentration, initially very narrow, increases with time and absorbs a higher potential drop (see curves corresponding to 1.0, 0.0 and 0.1 ps in Figs. 5 and 6), so that the point at which the potential reaches V_{th} moves well inside the recess-drain region after some time. When this happens, carriers injected from the recess will be mostly very fast carriers in the Γ valley which, having been accelerated by the high field in the recess region, have not reached the L valley because of the lower potential drop. These fast Γ carriers progressively fill (0.2-0.6 ps) the depleted region previously described until achieving the uniform carrier concentration of the starting conditions at 0.7 ps.

The peak in the electric field observed in Fig.4 takes place at the low-concentration region, and moves towards the drain at the very high velocity of the Γ valley electrons filling the depleted region (10×10^7 cm/s). That is the reason for the ultra-fast motion of the high-field region (Fig. 4) and the associated current oscillations. While L-electrons are being injected into the recess-drain region and the depleted region is increasing, the current decreases, for then growing when only Γ-electrons are injected from the recess.

Once the threshold of 0.6 V is surpassed, as the applied voltage increases, the formation of the depleted region requires more time, since it takes longer to move the V_{th} value of the potential far from the recess-drain edge to improve the Γ-valley injection. For the same reason, the depleted region is more pronounced. This explains the lower frequency and higher amplitude of the oscillations observed in Fig. 3 as the applied voltage increases.

It is important to remark that this ultra-high frequency non-stationary phenomenon is rather different to the classical Gunn effect, which is based in the propagation of a dipolar domain always traveling at the electron saturation velocity, slightly higher than 1×10^{7} cm/s in InGaAs, and therefore a much slower process. The ultra-fast quasi-ballistic Γ electrons at the origin of the oscillations found in the planar heterostructures appear as a consequence of: (i) the high electric field in the region under the recess and (ii) the degeneracy of the electron gas in the channel, which much reduces the emission of optical phonons (providing electron mobilities in excess of 15000 cm^{2}/Vs), so that electrons injected into the drain region are nearly ballistic. Even if some of these effects could be overestimated in our simulations (i.e. higher mobilities and velocities than in the experimental devices), all the conditions necessary for the onset of this ultra fast Gunn-like effect can be achieved in high mobility III-V heterolayers with submicrometer recess lengths. However, for the moment a clear experimental confirmation of this effect is still lacking, which is not an easy task due to the very high frequencies involved.

IV. CONCLUSIONS

This paper proposes a new source of THz radiation obtained from a novel ultra fast Gunn-like effect happening in planar AlGaAs/InGaAs slot diodes. An ensemble MC simulation has been used to investigate the oscillations that emerge when the bias of the slot diode surpasses a threshold voltage given by the Γ-L intervalley energy. At this point a kink appears in the I-V static characteristics and the instantaneous values of the current exhibit a coherent time-varying behavior at extremely high frequency, leading to a pronounced peak in its spectrum. It is demonstrated that THz frequencies are reached because of the presence of ultra-fast Γ electrons in the region of interest, effect achieved by means of the recess, which concentrates the voltage drop and injects very fast electrons into the drain region. Such ultra fast quasiballistic electrons appear mainly because of the degeneracy in the channel, which significantly reduces the rate of scattering mechanisms and much increases the electron mobility. From the practical point of view, it is interesting that a simple frequency tuning of the THz radiation is possible by means of the applied voltage. These oscillations have also been found in the simulations of InAlAs/InGaAs HEMTs with the same layer structure in open channel conditions, situation obtained for high gate-source voltages.

In order to exploit the full potentiality of these ultra fast Gunn-like diodes for the development of new THz MMICs it would be interesting to study the dependence of the frequency and magnitude of the oscillations on different geometrical and technological parameters, as the lengths of the recess and recess-drain regions, δ-doping, etc. This subject will be the objective of forthcoming works.

ACKNOWLEDGMENTS

This work has been partially supported by the projects TEC2007-61259/MIC from the Dirección General de Investigación (and FEDER) and SA044A05 from the Consejería de Educación y Cultura de la Junta de Castilla y León.

REFERENCES

[1] *Terahertz Frequency Detection and Identification of Materials and Objects,* edited by R.E. Miles, X.-C. Zhang, H. Eisele, A, Krotkus, *Springer*, 2007.

[2] R. Köhler, A. Tredicucci, F. Beltram, H. E. Beere, E. H. Linfield, A. G. Davies, D. A. Ritchie, R. C. Iotti and F. Rossi, Nature 417, 156 (2002).

[3] G.L. Carr, M.C. Martin, W.R. McKinney, K. Jordan, G.R. Neil and G.P. Williams, Nature **420,**153 (2002).

[4] J. Łusakowski, W. Knap, N. Dyakonova, L. Varani, J. Mateos, T. Gonzalez, Y. Roelens, S. Bollaert, A. Cappy, and K. Karpierz, J. Appl. Phys. **97**, 64307 (2005).

[5] N. Dyakonova, A. El Fatimy, J. Łusakowski, .W. Knap, M. I. Dyakonov, M. A. Poisson, E. Morvan, S. Bollaert, A. Shchepetov, Y. Roelens, Ch. Gaquiere, D. Theron, and A. Cappy, Appl. Phys. Lett. **88,** 141906 (2006).

[6] M. Dyakonov and M. Shur, Phys. Rev. Lett. **71**, 2465 (1993).

[7] J. Mateos, S. Pérez, D. Pardo and T. González, *2006 International Conference on Indium Phosphide and Related Materials Conference Proceedings*, ,IEEE Proceedings, 313, 2006

[8] S. Pérez, J. Mateos, D. Pardo, T. González, *Noise and Fluctuations*, Edited by M. Tacano, Y. Yamamoto, M. Nakao, *AIP Conference Proceedings,* **922,** 197 (2007)

[9] G. M. Dunn, A. Phillips and P. J. Topham, Semicond. Sci. Technol. **16**, 562 (2001).

[10] A. Khalid, N. J. Pilgrim, G. M. Dunn, M. C. Holland, C. R. Stanley, I. G. Thayne, and D. R. S. Cumming, IEEE Trans. Electron. Dev. **28**, 849 (2007).

[11] J. Mateos, T. González, D. Pardo, V. Hoel and A. Cappy, IEEE Trans. Electron. Dev. **47**, 250 (2000).

[12] J. Mateos, T. González, D. Pardo, V. Hoel and A. Cappy, IEEE Trans. Electron. Dev. **47**, 1950 (2000).

FIGURE CAPTIONS

Fig. 1. Geometry of the simulated InAlAs/InGaAs slot diode (Note that *X* axis is used in Figs. 4, 5 and 6).

Fig. 2. (a) Static I-V characteristic of the slot diode. The insets show the time-varying current for different applied voltages: $V_{DS} \leq 0.6$ V –left inset- $V_{DS} > 0.6$ V –right inset. (b) and (c) Spectral density of current fluctuations for V_{DS}=1.0 V and V_{DS}=0.1 V, respectively.

Fig. 3. Amplitude (crosses, left axes) and frequency (triangles, right axes) of the main peak in the spectral density of current fluctuations as a function of V_{DS}. Dotted lines indicate the V_{DS} regime where Gunn oscillations take place.

Fig. 4. Profile of the longitudinal electric field in the channel of the heteroestructure at different time moments within one period of the oscillation for a bias V_{DS}=1.0 V. The insets show the time-varying current during one period of the oscillation.

Fig. 5. (a) Profile of the carrier concentration in the channel of the heteroestructure at different time moments within one period of the oscillation for a bias V_{DS}=1.0 V.

(b) Profile of the Γ- valley (dotted line), L-valley (dashed line) and total carrier concentration (solid line) in the channel at time 0.0 ps.

Fig. 6. Profile of the potential in the channel of the heteroestructure at different time moments within one period of the oscillation for a bias V_{DS}=1.0 V. The point corresponding to V_{th}=0.6 V is marked in the different curves.

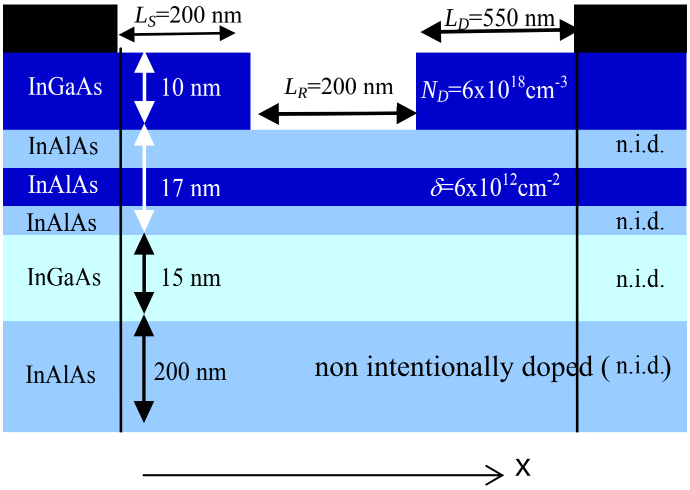
L_S=200 nm
L_D=550 nm
InGaAs
10 nm
L_R=200 nm
N_D=6x10^{18}cm^{-3}
InAlAs
n.i.d.
InAlAs
17 nm
δ=6x10^{12}cm^{-2}
InAlAs
n.i.d.
InGaAs
15 nm
n.i.d.
InAlAs
200 nm
non intentionally doped (n.i.d.)
x

.

Fig.1

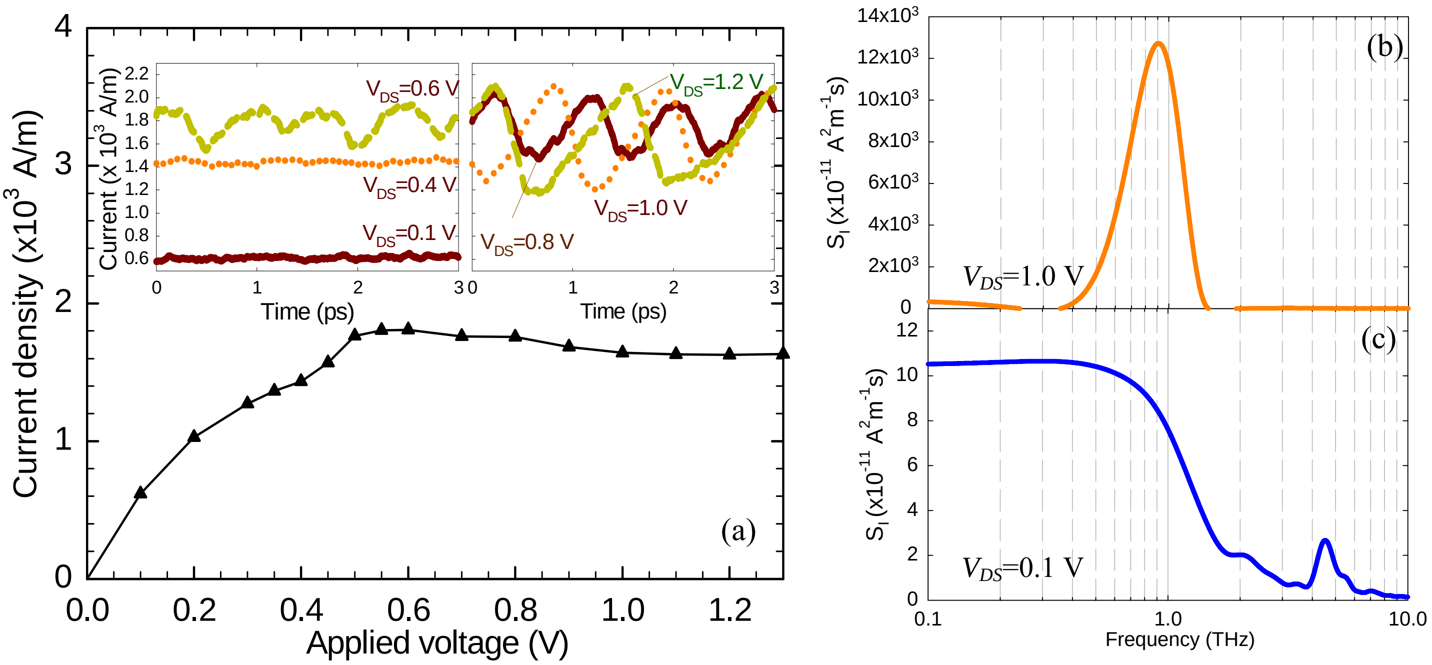
(a)
Current density (x10^3 A/m)
Applied voltage (V)
0
1
2
3
4
0.0
0.2
0.4
0.6
0.8
1.0
1.2
Current (x 10^3 A/m)
2.2
2.0
1.8
1.6
1.4
1.2
1.0
0.8
0.6
Time (ps)
0
1
2
3
V_{DS}=0.6 V
V_{DS}=0.4 V
V_{DS}=0.1 V
V_{DS}=1.2 V
V_{DS}=1.0 V
V_{DS}=0.8 V
(b)
S_I (x10^{-11} A^{2}m^{-1}s)
14x10^3
12x10^3
10x10^3
8x10^3
6x10^3
4x10^3
2x10^3
0
V_{DS}=1.0 V
(c)
S_I (x10^{-11} A^{2}m^{-1}s)
12
10
8
6
4
2
0
V_{DS}=0.1 V
0.1
1.0
10.0
Frequency (THz)

Fig.2

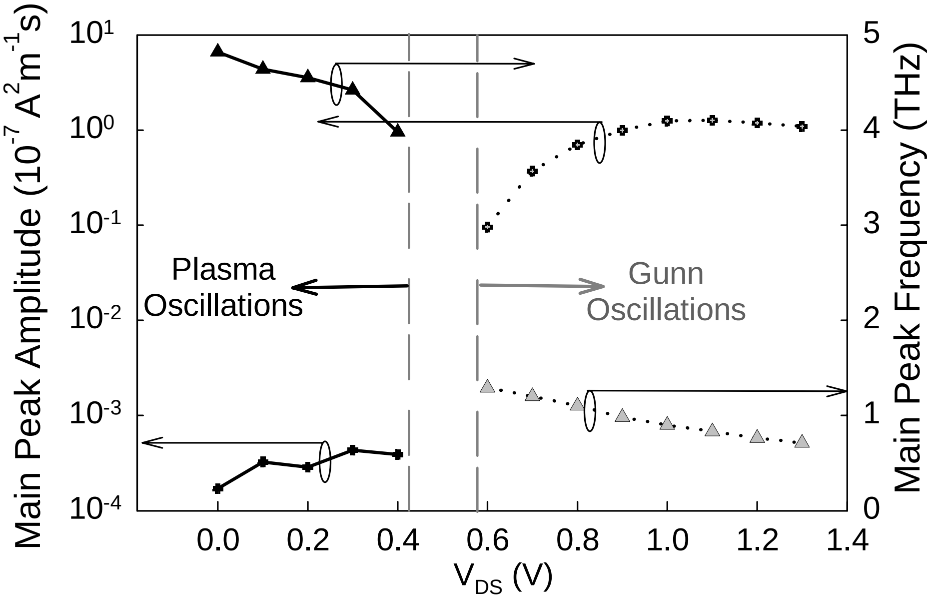
Main Peak Amplitude (10^-7 A^2 m^-1 s)
10^1
10^0
10^-1
10^-2
10^-3
10^-4
Main Peak Frequency (THz)
5
4
3
2
1
0
0.0
0.2
0.4
0.6
0.8
1.0
1.2
1.4
V_DS (V)
Plasma Oscillations
Gunn Oscillations

Fig. 3

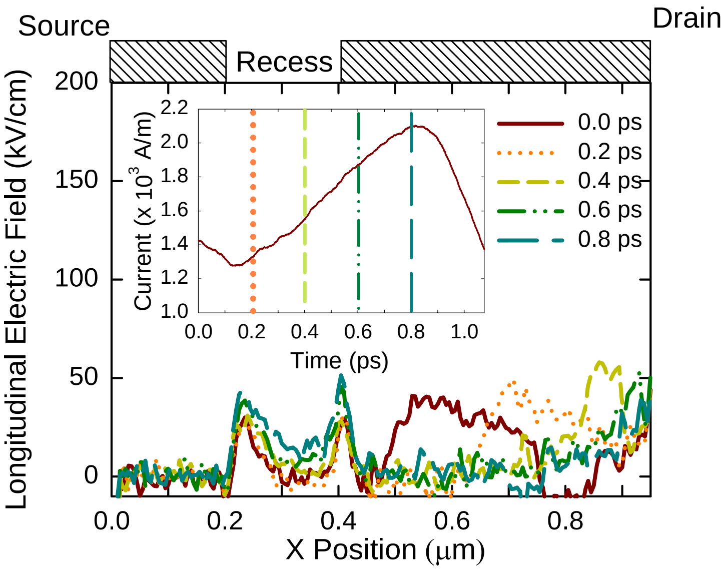
Source
Recess
Drain
Longitudinal Electric Field (kV/cm)
200
150
100
50
0
0.0
0.2
0.4
0.6
0.8
X Position (μm)
Current (x 10^3 A/m)
2.2
2.0
1.8
1.6
1.4
1.2
1.0
0.0
0.2
0.4
0.6
0.8
1.0
Time (ps)
0.0 ps
0.2 ps
0.4 ps
0.6 ps
0.8 ps

Fig. 4

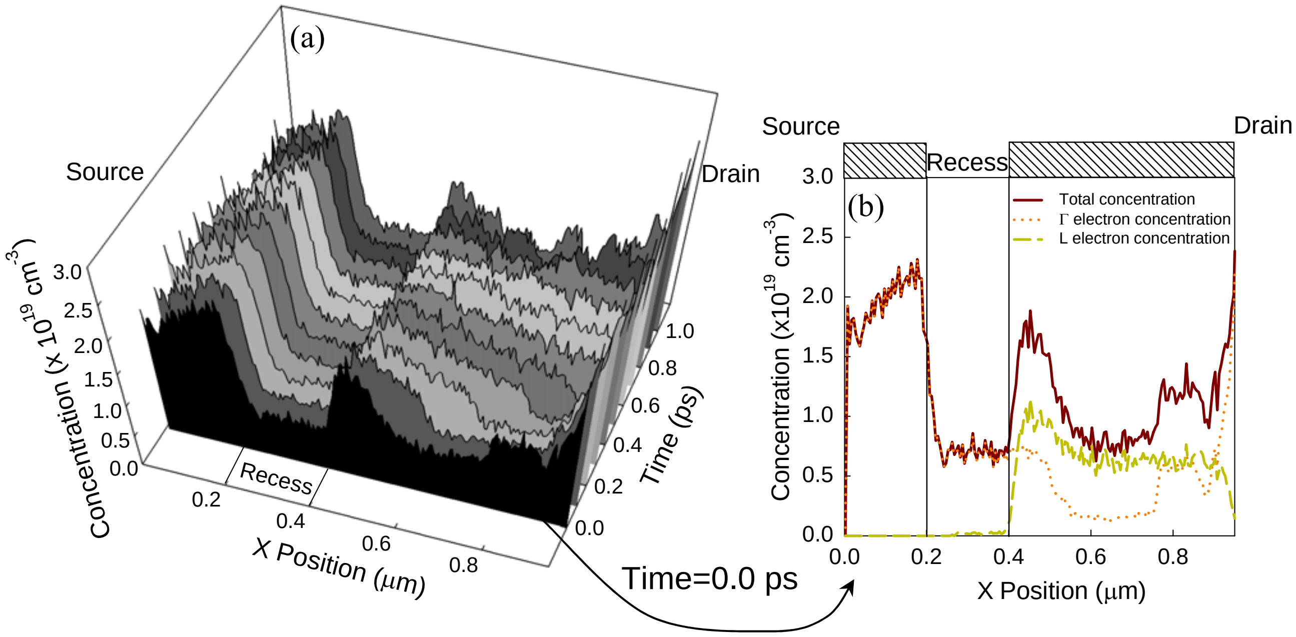
(a)
Source
Drain
Concentration (x 10^{19} cm^{-3})
3.0
2.5
2.0
1.5
1.0
0.5
0.0
Recess
0.2
0.4
0.6
0.8
X Position (μm)
Time (ps)
0.0
0.2
0.4
0.6
0.8
1.0
Time=0.0 ps
(b)
Source
Recess
Drain
Total concentration
Γ electron concentration
L electron concentration
Concentration (x10^{19} cm^{-3})
3.0
2.5
2.0
1.5
1.0
0.5
0.0
0.0
0.2
0.4
0.6
0.8
X Position (μm)

Fig.5

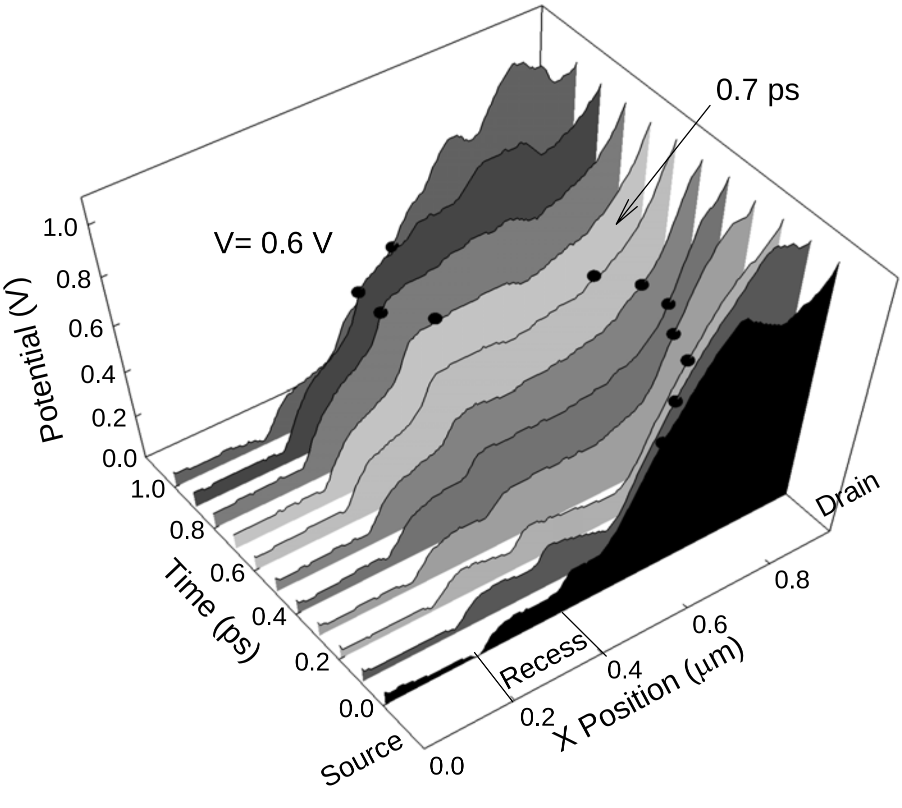
0.7 ps
V= 0.6 V
Potential (V)
1.0
0.8
0.6
0.4
0.2
0.0
Time (ps)
1.0
0.8
0.6
0.4
0.2
0.0
Source
Recess
Drain
X Position (μm)
0.0
0.2
0.4
0.6
0.8

Fig.6